Electronic Supplementary Material (ESI) for Lab on a Chip.

Charge-controlled microfluidic formation of lipid-based single- and multicompartment systems

Barbara Haller,[ab] Kerstin Göpfrich,[ab] Martin Schröter,[ab] Jan-Willi Janiesch,[ab] Ilia Platzman,[*ab] and Joachim P. Spatz[*ab]

[a]Department of Cellular Biophysics, Max Planck Institute for Medical Research, Jahnstraße 29, 69120 Heidelberg, Germany

[b]Department of Biophysical Chemistry, University of Heidelberg, Im Neuenheimer Feld 253, 69120 Heidelberg, Germany

KEYWORDS: synthetic cell, microfluidics, water-in-oil-droplets, giant unilamellar vesicles, fluorosurfactants, compartments

Correspondence: Spatz@mf.mpg.de, Ilia.Platzman@mpimf-heidelberg.mpg.de

Supplementary data and figures

DLS

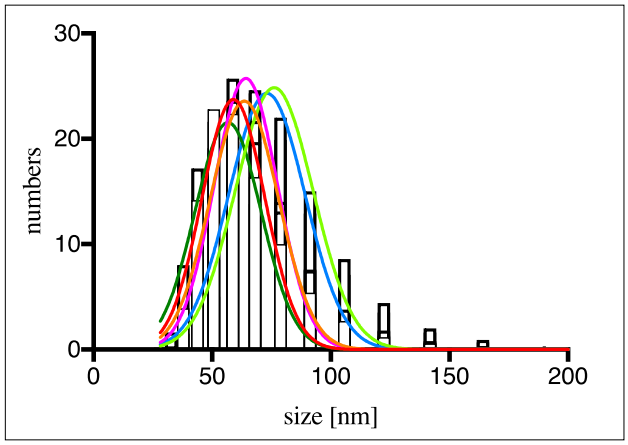

Figure S1. Size distribution of SUVs measured by DLS. Histogram indicates the mean distribution of 6 measurements (mean diameter: 68 ± 15 nm)

Microfluidic Devices

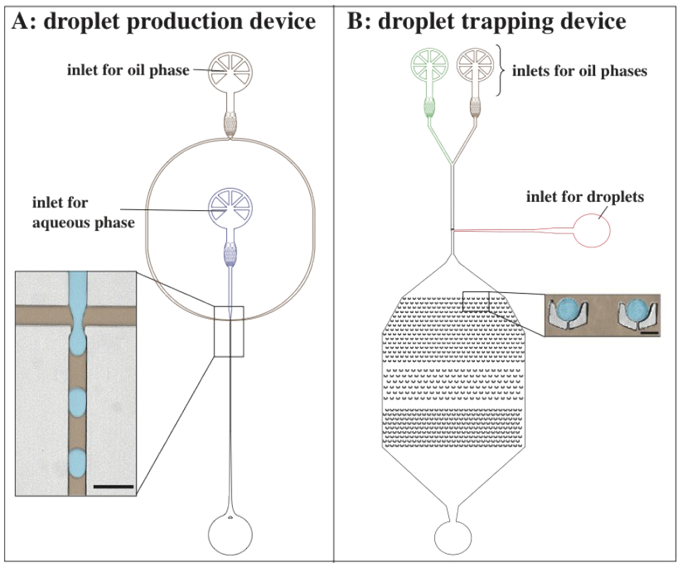

Figure S2. Schematic representation of the droplet-based microfluidic devices that were implemented in this research. (A) Droplet production device containing an aqueous and an oil inlets. The insert shows a representative bright-field image of the flow-focusing junctions for droplet production with a diameter of 30 µm. In sake of clarity of presentation aqueous and oil phases were colored in blue and brown, respectively. B) Droplet trapping device containing one inlet for droplets and two inlets for oil. The trapping unit consists of V-shaped cavities to keep droplets in place during time-lapse observation. The insert shows a representative bright-field image of droplets trapped in cavities of the observation unit. In sake of clarity of presentation droplets and oil phase were colored in blue and brown, respectively. Scale bars 50 µm.

FTIR

A *B*

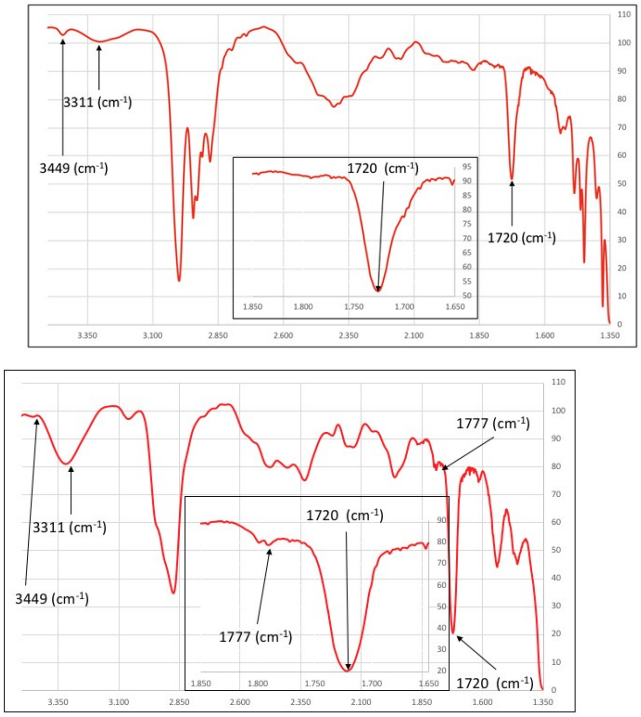

Figure S3. A and B present FTIR spectra of perflouro-polyether-polyethylene glycol (PFPE-PEG) block-copolymer fluorosurfactants (PEG-based fluorosurfactants) containing 10% surfactants in HFE-7500 oil and pure surfactants, respectively. Both spectra show absorption peaks at 3449 cm-1and 3311 cm-1 corresponding to the symmetrical and unsymmetrical stretching vibration of primary amines. The band at 1720 cm-1 is attributed to a stretching mode of the (C=O) band of the amid group which connects the PEG-diamine with the Krytox. The bands in figure A between 2999 cm-1and 2875 cm^{-1} are attributed to symmetric and asymmetric stretching modes of the PEG (C-H) groups, respectively. In figure B (pure Surfactant) the bands of the PEG (C-H) overlap to one broad band. In figure be an additional tiny band is visible at 1777 cm^{-1} representing traces of the stretching mode of the (C=O) band of the carboxylic acid group of the Krytox educt.

MALDI-TOF

A further characterization of the PEG-based fluorosurfactant was performed by MS (MALDI-TOF) measurements. In figure S4 the region around 2000 m/z is increased (B) showing a series of peaks with the mass difference of 166 (region 1, shown in blue). This mass difference correlates exactly with the molecular weight of PFPE monomers. Thus, the presence of Krytox molecules with a molecular weight of around 2000 Da could be confirmed. In m/z regions II and III a series of peaks with the mass difference of a PEG- (44 Da) plus PFPE- (166 Da) monomer was observed, referring to a wide size range of PFPE-PEG block-copolymers between 3500 Da and 6500 Da. Based on the Krytox pattern in region I of around 2000 Da, it can be assumed that the fluorosurfactant consists of a mixture of di- and triblock-copolymer, with an average molecular weight of around 4000 Da and 6000 Da, respectively. This means, that depending on the ratio between di- and triblock-polymer, a 1.4 wt% solution of the surfactant in HFE-7500 (ρ = 1.61 g/ml)

has a molar concentration between 3.8 mM (100 % triblock-polymer) and 5.7 mM (100 % diblock-polymer). Note that for the calculation of surfactant concentration, the amount of Krytox was ignored.

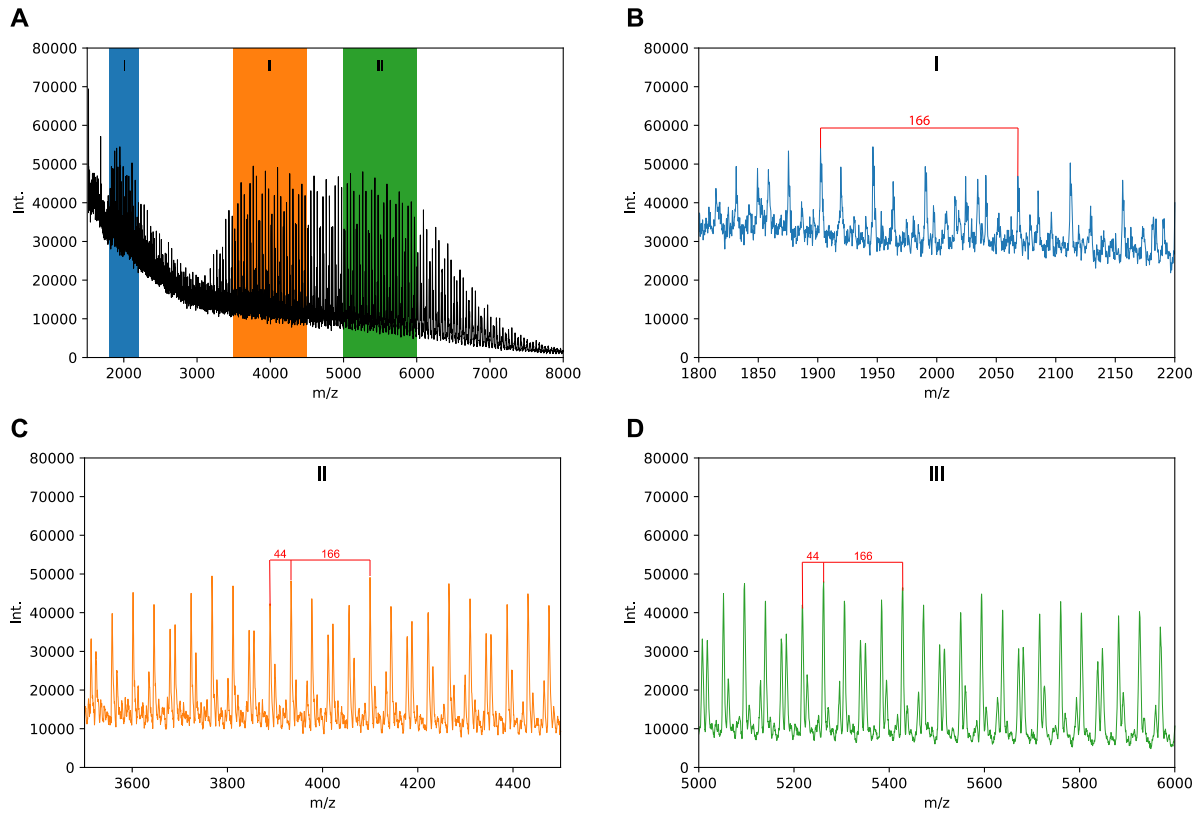

Figure S4. MS (MALDI-TOF) measurement of PEG-based fluorosurfactant. A: Complete spectrum in m/z range of 1500 to 8000. B: Spectrum of region I with a mass pattern of PFPE polymer (OCF(CF3)CF2, Δm = 166) referring to Krytox molecules of around 2000 Da. C: Spectrum of region II showing the MW of diblock-polymers with mass differences of PFPE/PEG monomers (OCF(CF3)CF2, Δm = 166 + OCH2CH2, Δm = 44). D: Spectrum of region III showing the MW of triblock-polymers with mass differences of PFPE/PEG monomers.

Partitioning experiment

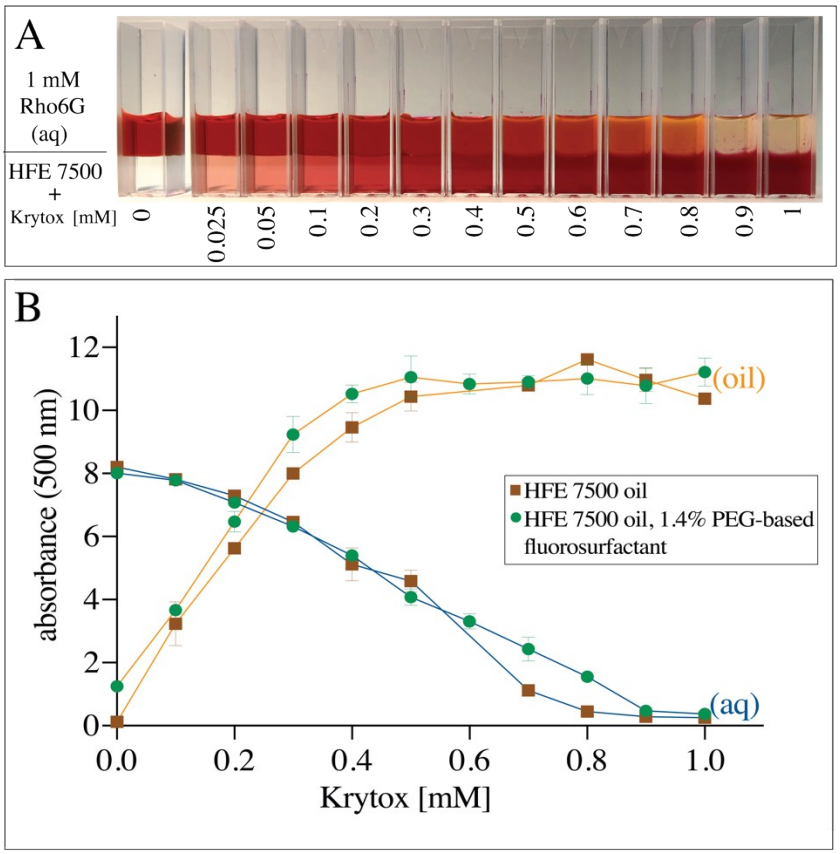

Figure S5. Representative images of the partitioning experiments and their analysis. A) Aqueous solutions of Rhodamine 6G 1 mM (upper phase) are exposed to the HFE 7500 oil phase containing Krytox at different concentrations (indicated at the bottom of the images) in a 3.5 ml cuvette. B) Spectrometric analysis (absorbance at 500nm) of Rhodamine 6G in aqueous (blue) and oil phases (yellow) after 48 h partitioning experiment. The Y-axis intercept of the samples containing 1.4 wt% PEG-based fluorosurfactants corresponds to Krytox traces in the PEG-based fluorosurfactant (in 1.4 wt% ~0,038 mM).

Release efficiency

To quantify the success rate of the release, an observation area of 246.5 x 20000 µm was screened for released GUVs and the efficiency was calculated. GUVs in the size range of 20 – 30 µm were counted (N_{count}). N_{count} values were used to interpolate the efficiency of the release process according to the following estimates:

Total volume: $V_{aq\_total} = V_{release\ buffer} + V_{aq\_encapsulated} = 83.3\ \mu l$

Total number of GUVs: $N_{GUVs,total} = N_{count} * (V_{aq\_total} / V_{aq\_count}) = N_{GUVs,\ count} * 187.8$

Efficiency of release: $E_{release}$ [%] = ($N_{GUVs,total}$ / N_{dsGUVs}) * 100

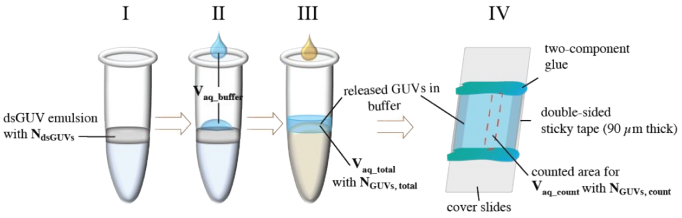

Figure S6. Calculating release efficiency. I. Collection of dsGUVs for 10 min with production rate of 4.2 kHz lead to 2.52 x 10^6 dsGUVs. II. Addition of aqueous buffer V_{buffer}. III. Addition of de-emulsifier to release GUVs into the aqueous phase. IV. Observation chamber made from two BSA-coated cover slides and a double-sticky tape as a spacer. Edges are sealed with two component glue. In a volume of 246.5 x 20000 x 90 µm (V_{aq_count}, marked in red) released GUVs were counted ($N_{GUVs,\ count}$) and total number of GUVs in V_{aq_total} was extrapolated.

Effect of Mg2+ concentrations and monovalent ions on interactions between SUVs and droplet interface

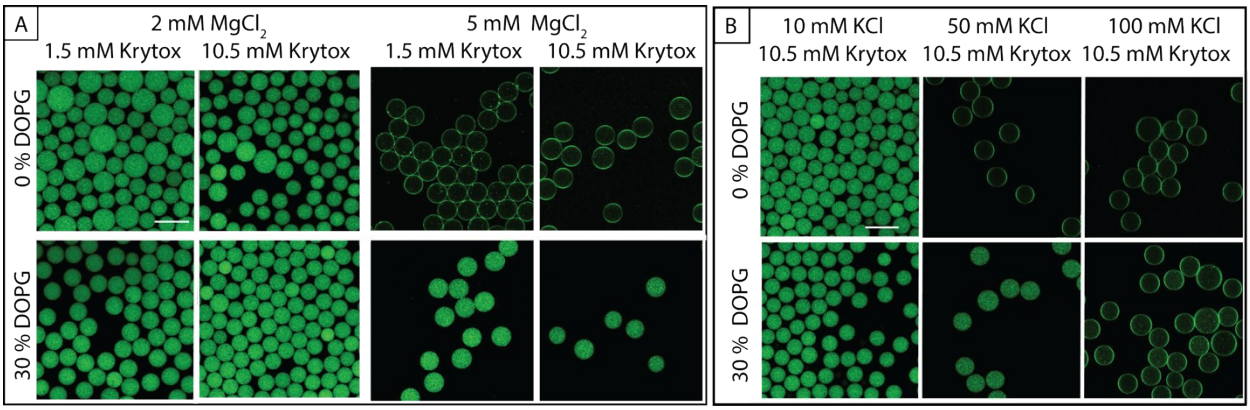

Figure S7: Representative images of green fluorescence from SUVs (DOPC 42.25 % or 27.25 %, POPC 42.25 % or 27.25 %, ATTO 488-labeled DOPE 0.5 %, cholesterol 15 % and DOPG 0 % or 30 %). (A) SUVs are dissolved in 30 mM Tris, pH 7.4 plus 2 mM or 5 mM $MgCl_2$ and droplets are stabilized by PEG-based fluorosurfactants (1.4 wt%) with 1.5 mM or 10.5 mM Krytox. Lipid interaction with the periphery could only be observed for neutral lipids in buffers containing 5 mM $MgCl_2$. (B) SUVs are dissolved in 30 mM Tris, pH 7.4 plus 10 mM, 50 mM or 100 mM KCl and droplets are stabilized by PEG-based fluorosurfactants (1.4 wt%) and 10.5 mM Krytox. Lipid interaction with the periphery could be observed for neutral lipids in buffers containing 50 mM and 100 mM and for a lipid composition containing 30 % negatively charged lipids in a buffer containing 100 mM KCl. Scale bar, 50 µm.

Compartments without mono- or bilvalent ions

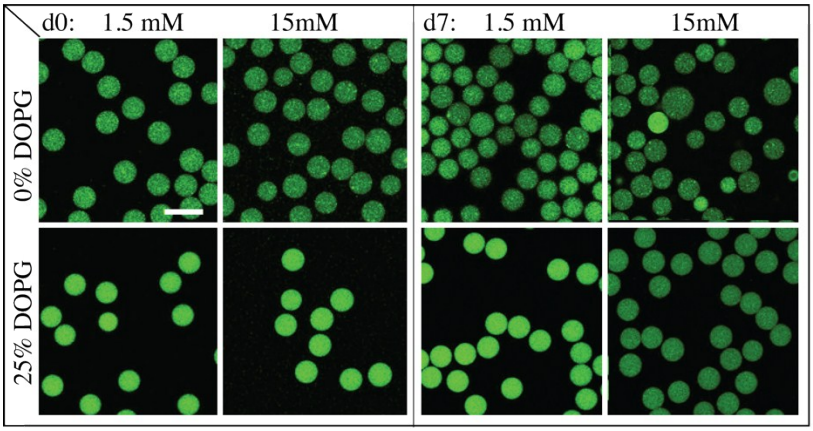

Figure S8. Representative images of homogeneously distributed green fluorescence from SUVs (DOPC 42.25 or 29.75%, POPC 42.25 or 29.75%, ATTO 488-labeled DOPE 0.5 %, cholesterol 15% and DOPG 0% or 25%) within the droplets generated in the oil phase containing PEG-based fluorosurfactants (1.4 wt%) and Krytox (1.5 mM or 15 mM). No generation of dsGUVs could be observed 1h after production or 7 days after production due to the absence of mono- or bivalent ions in Tris buffer. Scale bar, 50 µm.

Time-lapse analysis of dsGUV formation

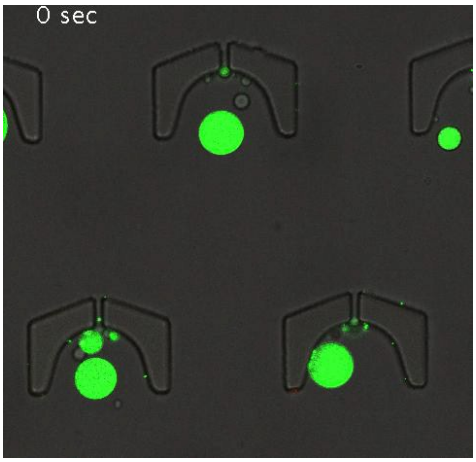

Video S1: Time-lapse analysis of dsGUV formation (DOPC 42.25%, POPC 42.25%, cholesterol 15% and 0.5% ATTO 488-labeled DOPE) in a microfluidic trapping device. Droplets are trapped in PDMS cavities by applying a constant flow of HFE-7500 oil containing PEG-based fluorosurfactants. After 55 s addition of HFE-7500 oil containing Krytox (9 mM). For clarity, the oil containing Krytox was labeled with 10 nM Nile red. After 110 s: Attraction of SUVs to the droplet periphery. After 165 s: The accumulation of lipids on the droplet periphery is visible as a bright ring in the confocal plane. This indicates successful dsGUV formation.

FRAP

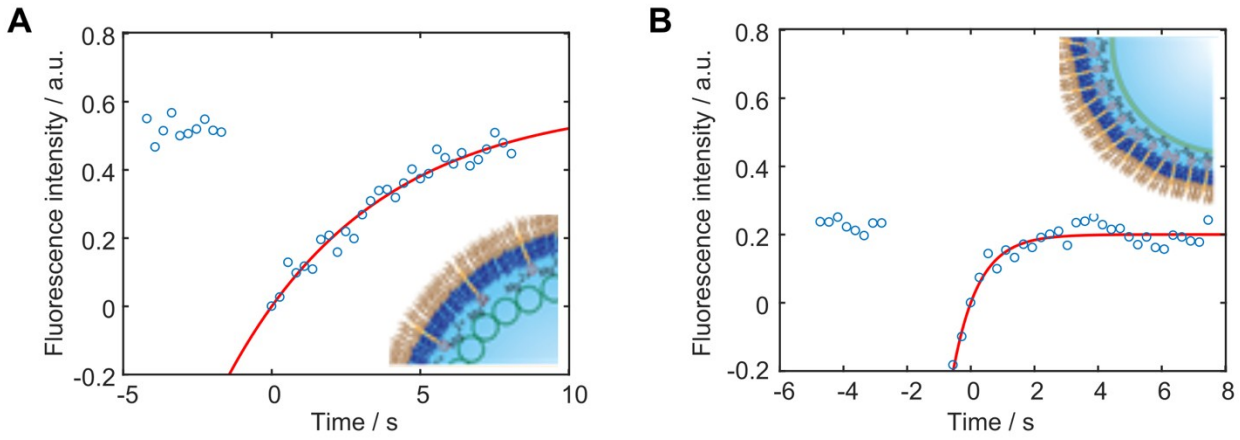

Figure S9. FRAP measurements of lipid diffusion in microfluidic droplets. Exemplary recovery traces show that it is possible to distinguish between A) multicompartment adhesion (D= 1.2 ± 0.2 µm²/s, n = 40) and B) dsGUVs (D= 5 ± 0.4 µm²/s, n = 80).

Table S1: Diffusion coefficients of lipids within water-in-oil droplets stabilized by different surfactant ratios

DOPG in %	c(Krytox) [mM]	Diffusion coefficient [µm²/s]		
0	1.5	1.1 ± 0.1	n=20	
0	3.0	1.3 ± 0.2	n=20	
0	7.5	4.8 ± 0.4	n=20	
0	10.5	5.1 ± 0.5	n=40	5.0 ± 0.4 µm²/s
0	15	5.1 ± 0.3	n=20	
30	1.5	1.0 ± 0.1	n=20	
30	7.5	5.4 ± 0.4	n=20	
30	10.5	4.2 ± 0.3	n=40	4.8 ± 0.3 µm²/s
30	15	5.5 ± 0.3	n=20	

Cryo-SEM analysis of freeze-fractured droplets

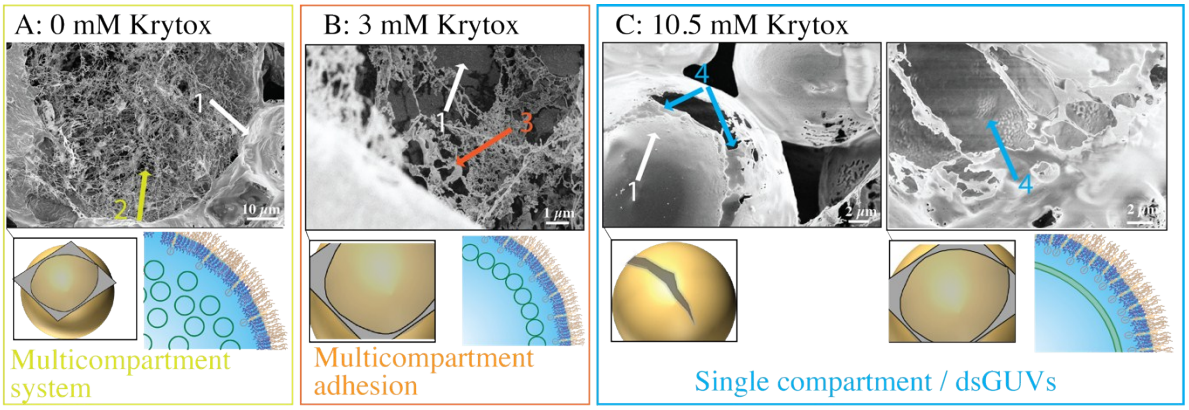

Figure S10: Representative cryo-SEM micrographs of freeze-fractured droplets. SUVs were encapsulated in droplets stabilized by 1.4 wt% PEG-based fluorosurfactant and 0 mM (A), 3 mM (B) and 10.5 mM Krytox (C). Arrows are indicating the surfactant shell (1), SUVs (2, 3) and lipid bilayer (4).

Neutral compartments after 7 days

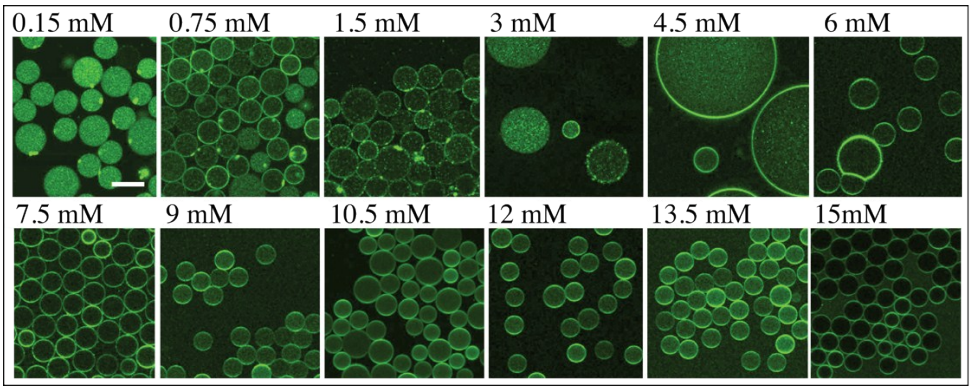

Figure S11. Representative images of green fluorescence from lipids (0.5 % ATTO 488-labeled DOPE) in the microfluidic droplets at day 7 after production. To evaluate the influence of Krytox on dsGUV formation and stability, different Krytox concentrations, indicated on top of the fluorescence images, were mixed with 1.4 wt% PEG-based fluorosurfactants in the oil phase. 10mM Mg^{2+} and SUVs comprised of 42.25% DOPC, 42.25% POPC and 15% cholesterol were used as an aqueous phase for droplets formation. Scale bar, 50 µm.

Compartments stabilized by high Krytox concentrations

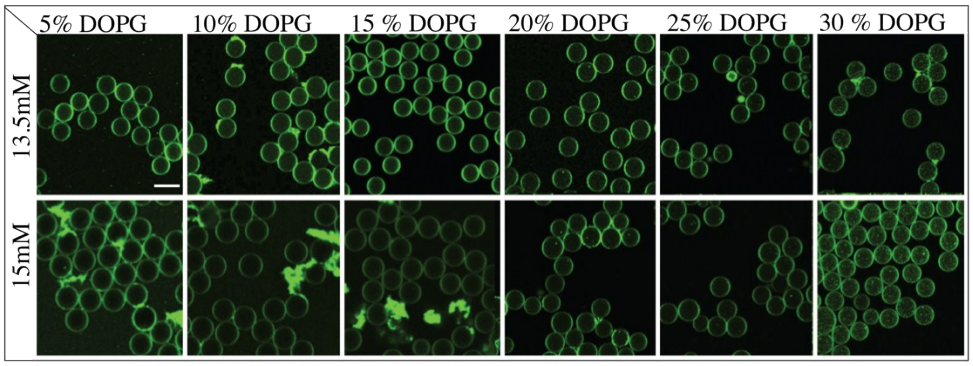

Figure S12. Representative images of green fluorescence from lipids (0.5 % ATTO 488-labeled DOPE) in the microfluidic droplets. To evaluate the influence of Krytox on dsGUV formation, different Krytox concentrations, indicated on top of the fluorescence images, were mixed with 1.4 wt% (weight) PEG-based fluorosurfactants in the oil phase. To evaluate the influence of negatively charged lipids on dsGUV formation, the Tris buffer including 10 mM Mg^{2+} and SUVs comprised of different ratios of negatively charged DOPG lipids (DOPC x%, POPC x%, DOPG 0% – 30%, cholesterol 15%) was used as an aqueous phase for droplets formation. Scale bar, 50 µm.

Lipid leakage depending on lipid charge

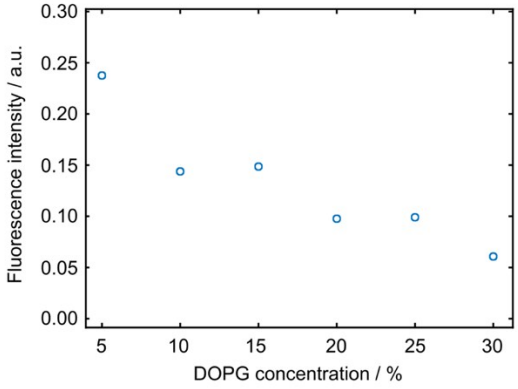

Figure S13. Quantification of lipid leakage from the water phase inside the droplet into the surrounding oil phase as a function of lipid charge. The fluorescence intensity from the lipids (0.5 % DOPE-Atto488) in the oil phase was normalized to the intensity in the water phase. Less lipid leakage is observed at higher concentrations of negatively charged lipids (DOPG) within the lipid mixture.

Size distribution of droplet-stabilized vs. released GUVs

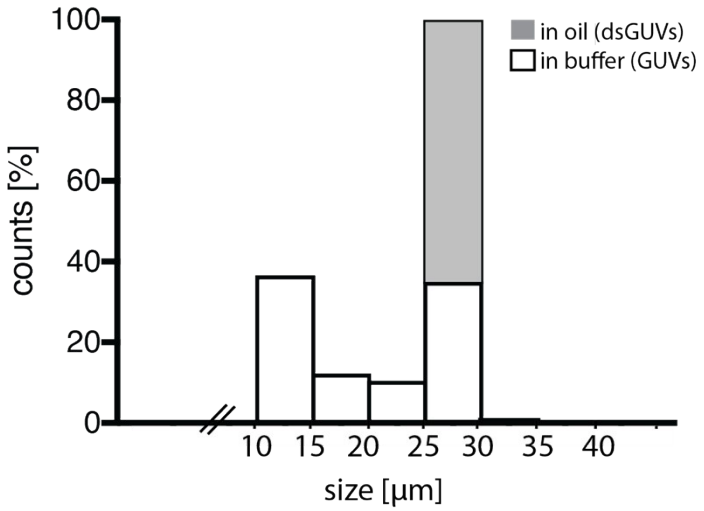

Figure S14: Size distribution of dsGUVs in the oil phase (grey column, n =187) and after the release into the water phase (GUVs, white columns, n = 190). The lipid composition comprises DOPC 27.25 %, POPC 27.25 %, ATTO 488-labeled DOPE 0.5 %, cholesterol 15 % and DOPG 30 %. Note that GUVs smaller than 10 µm were not taken into account.

Fluorescence intensity profiles of a single and a multicompartment system

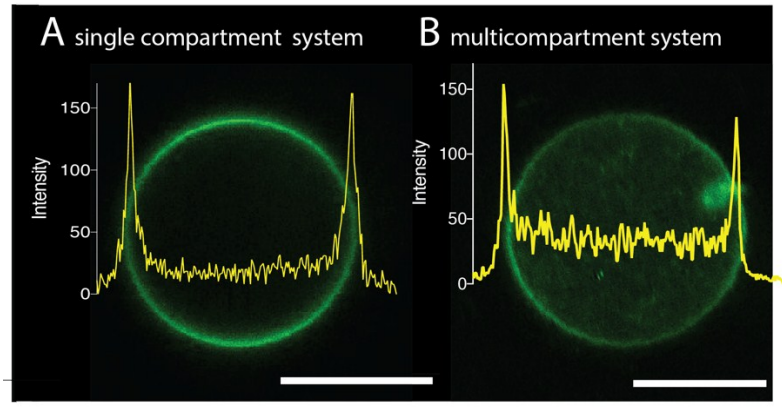

Figure S15: Representative confocal fluorescence images of (A) a single and (B) a multicompartment system released into the water phase. Images were taken under the same acquisition conditions. Fluorescent intensity profiles along the cross section of the GUVs are plotted in yellow. Fluorescence signal of 0.5 % Alexa 488-labelled DOPE lipids in the lipid compositions (DOPC 27.25 %, POPC 27.25 %, ATTO 488-labeled DOPE 0.5 %, cholesterol 15 % and DOPG 30 %). Scale bars, 10 µm.